Materials Today Bio 32 (2025) 101722

Contents lists available at ScienceDirect

Materials Today Bio

journal homepage: www.journals.elsevier.com/materials-today-bio

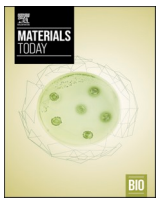

Drug-free hyaluronic acid-microneedle with unexpected inhibition activity on benzalkonium chloride-induced corneal inflammation and stromal scarring

Baoshan Huang [a,b,1], Rui Zeng [a,1], Xiao Liu [a,1], Lu Pan [a], Haitong Bai [a], Jiachen Liao [a], Wenkai Xu [a], Hong Fu [a], Kaihui Nan [a,b,*], Sen Lin [a,b,**]

[a] National Engineering Research Center of Ophthalmology and Optometry, Eye Hospital, Wenzhou Medical University, Wenzhou, 325027, China
[b] School of Biomedical Engineering, Wenzhou Medical University, Wenzhou, 325027, China

ARTICLE INFO

Keywords:
Microneedle
Hyaluronic acid
Artificial tear
Dry eye disease
Corneal stromal scarring

ABSTRACT

Topical instilling of commercial artificial tears (cAT, containing 0.1 % hyaluronic acid) is widely employed to alleviate clinical manifestations of mild dry eye disease (DED) by preventing the pathological change of corneal epithelium. However, it showed limited therapy effectiveness on heavy DED which has further involved corneal stroma, due to its low stroma-available for hyaluronic acid (HA) resulting from the barrier of corneal epithelium. The present study developed a new microneedle-dosage form of cAT (cAT-MN). This cAT-MN can overstride the corneal epithelium and act as a long-lasting protective agent. Compared to cAT dosing (4 times/day), cAT-MN with one treatment exerted significantly higher therapeutic effects on curbing benzalkonium chloride (BAC)-induced corneal stroma scaring as well as alleviating the DED symptoms in the first 5-day BAC exposure; whereas, showed limited effects in a 10-day BAC exposure. To expand the therapy effects, MNs containing various amounts of HA were prepared. Thereinto, HA(6 %)-MN recovered corneal damage to healthy levels, which could be attributed to adding stroma-available for HA both by increasing the amounts of HA-delivery and enhancing HA-permeation. This study explores a new drug-free microneedle-dosage form of cAT to cure corneal stroma disorders which has expanded its indication, promising a wide clinical use in ophthalmology.

1. Introduction

Artificial tears are the most consummated eye drops clinically to manage mild dry eye disease (DED) by supplementing either the aqueous or lipid part of the tears [1]. The components of commercial artificial tears can be varied from products depending on their purpose. Hyaluronic acid (HA), a glycosaminoglycan naturally occurring in extracellular matrix and tissues, is a common constituent in several commercial artificial tears [1,2]. The HA can relieve DED-related symptoms (e.g. inflammation, corneal edema …) by adding moisture and lubrication to the cornea. Chemically, each HA molecule contains a reducing terminal saccharide residue and thus could act as a significant antioxidant [3,4]. This contributed to DED therapy by inhibiting oxidative damage of cornea epithelium [5–7]. However, topical administration of artificial tears showed limited therapy effectiveness on heavy DED which has further involved corneal stroma damages, due to its low stroma-available resulting from the barrier of corneal epithelium. The corneal epithelium which constitutes the lamellar structure of the cornea together with the endothelium, Descemet's membrane, stroma, and Bowman's layer, is naturally present at the outermost of the eye [8]. Corneal epithelium serves as the first-line physical barrier that separates the inside and outside of the eye, protecting the eye from disturbing of external environment and facilitating intraocular homeostasis [9]; however, it also acts as a significant obstacle to intraocular drug delivery. We previously developed peptide-modified nano-micelle [10], multi-hydrophobic-core nanoparticles [11], and precorneal depot [12]

* Corresponding author. National Engineering Research Center of Ophthalmology and Optometry, Eye Hospital, Wenzhou Medical University, Wenzhou, 325027, China.
** Corresponding author. National Engineering Research Center of Ophthalmology and Optometry, Eye Hospital, Wenzhou Medical University, Wenzhou, 325027, China.
E-mail addresses: nankh@wmu.edu.cn (K. Nan), lin_sen@wmu.edu.cn (S. Lin).
[1] These authors contributed equally to this work.

https://doi.org/10.1016/j.mtbio.2025.101722
Received 25 February 2025; Received in revised form 26 March 2025; Accepted 29 March 2025
Available online 29 March 2025

to overcome these onsite biological barriers. These strategies are largely based on in-direct ways by prolonging drug retention on the ocular surface and enhancing tissue permeability. Despite their promise, these methods still showed unsatisfactory improvement in the bioavailability of the drugs. Microneedles (MNs) representing a minimally invasive and patient-friendly device to break through solid biological barriers have emerged for efficient drug delivery [13–15]. It can act as micro-depots for sustainable drug release in target tissues. These characteristics make it suitable for ocular surface medication by remarkedly improving bioavailability and reducing application frequency (compared to eye-drop) [13]. We assumed that it could increase stroma-available for the active components within artificial tears by developing a microneedle-dosage form of commercial artificial tears (cAT-MN), thus consequent favorable therapeutic effects against corneal stromal disorders. Compared to traditional stromal injection (the drug was confined to the injection site), the MN delivered the therapeutic agents into the stroma in an array form (depending on the design of the MN array), which could gain a better outcome in the management of the diffused corneal stromal disorders.

Corneal stroma makes up about 90 % of the corneal thickness [8]. It is an aligned collagen fiber structure with optical clarity. Any damage to the corneal stroma can lead to corneal scarring and sight-threatening [8]. One possible iatrogenic contributor to corneal stromal scaring is the overdose of preservatives in ophthalmological solutions [16]. Benzalkonium chloride (BAC), a quaternary ammonium compound, is a broad-spectrum antiseptic and germicide against bacteria, fungi, and viruses. BAC is the most widely employed as a preservative in ophthalmic formulas [17–19]. Chronic repeating exposure to BAC can induce ocular surface damage including corneal epithelial cell apoptosis and conjunctival goblet cell loss [20,21]. And further causes lymphocyte and inflammatory cell infiltration to the stroma that leads to corneal stromal scaring [22–24]. It is necessary to explore new treatments for BAC-induced corneal inflammation and stromal scarring.

We hypothesized that the microneedle which can overstride the corneal epithelium barrier could deliver commercial artificial tear to corneal stroma effectively; and thus act as an in situ long-lasting cornea protection agent. We first tried to fabricate the cAT-MN by casting artificial tears (containing 0.1 % HA) directly. However, it failed to demolding. To facilitate cAT-MN preparation, it is necessary to extra-fill additional polymer (as an excipient) to commercial artificial tears. Water-soluble poly (vinyl alcohol) (PVA) is an FDA-approved biocompatible polymer with desirable mechanical properties for microneedle patch preparation [25,26]. Considering these factors, a new dissolving cAT-MN was prepared by dissolving PVA into the artificial tear solution; and fabricated using molding-casting technology. The therapy effects of cAT-MN and cAT on BAC-induced corneal damage were compared (Fig. 1). To further elaborate the effects of HA, dissolving MNs containing various amounts of HA were prepared. The HA(6 %)-MN could recover stromal scarring and DED symptoms to healthy levels. Further investigation revealed that the HA(6 %)-MN could suppress the ox-mtDNA/NLRP3/IL-1β pathway, which contributed to its therapy effects on BAC-induced corneal injury (both in the epithelium and the stroma). The present study explores a new drug-free microneedle-dosage form of commercial artificial tears to cure corneal stroma disorders which have expanded its indication, promising a wide clinical use in ophthalmology.

2. Materials and methods

2.1. Materials

Sodium hyaluronate (HA, MW = 400 kDa, determined by gel permeation chromatography) was obtained from Bloomage Biotech (China). The commercial artificial tears (HYLO COMOD®, contains 0.1 % of HA) were bought from URSAPHARM Arzneimittel GmbH (Germany). Polydimethylsiloxane (PDMS, Sylgard 184) was purchased from Dow Corning (Midland, MI). Benzalkonium chloride (BAC), polyvinyl alcohol (PVA), N-hydroxysuccinimide (NHS), and 1-ethyl-3,3-dimethylaminopropyl carbodiimide (EDC) were acquired from Sigma-Aldrich (USA). Cy5.5 amine was purchased from MeloPEG (China). The human corneal epithelial cells (HCECs) were obtained from ATCC (USA).

2.2. Fabrication of HA-MN patches

The HA-MN patches were fabricated using the molding-casting method. PDMS micromolds were created by pouring PDMS solution into the 3D-printing resin master-molds (BMF Precision Tech Inc., China) and curing on a heating platform at 80 °C for 2 h. To fabricate commercial artificial tear microneedle (cAT-MN), 99 mg of PVA was dissolved in 1 mL of HYLO COMOD® artificial tears (contains 0.1 % of HA) obtaining a pre-casting solution with a total polymer content of 10 %. The pre-casting solution (100 μL) was then poured into a PDMS mold. The cAT-MN was harvested after a process of centrifugating (3500 rpm, 10 min), drying (37 °C, 12 h), and hand-demolding under stereo microscope (SZ650, Optec, China). To obtain HA-MN patches with different HA content, pre-casting solutions with different HA and PVA proportions (10 % of total polymer content) were prepared, and the HA-MN patches were obtained using the above-mentioned process.

2.3. Characterization of HA-MN patches

The morphology of HA-MN patches was recorded by a stereo-optical microscope (SZ680, Optec, China) and a scanning electron microscope (SEM, Phenom Pharos LE, ThermoFisher Scientific). Their mechanical compression properties were evaluated by a texture analyzer (CTX, AMETEK Brookfield, USA) under vertical compression mode. The MN patches were fixed on a rigid stainless-steel platform. The cylindrical probe (cross-sectional diameter: 1 cm) was approached to the MNs vertically with a speed of 0.1 mm/s. The changes of stress in a compression displacement of 0–0.5 mm were recorded. The tensile properties of the substrate of those MN patches were determined using the AMETEK Brookfield texture analyzer (equipped a clamp probes) at a tensile speed of 0.1 mm/s. The changes of stress in a tensile displacement of 0–15 mm were recorded.

2.4. Ex vivo and in vivo cornea insertion test of HA-MN patches

Female Sprague-Dawley rats (S/D rats, ~150 g) were obtained from the Experimental Animal Center of Wenzhou Medical University. All animal experiments were reviewed and approved by the Ethical Review Committee of the eye hospital of Wenzhou Medical University (EHWMU20240106) according to the National Research Council's Guide for the Care and Use of Laboratory Animals. Animals without infection on the eye surface and obstacle keratoleukoma were selected for the experiments. To evaluate the *ex vivo* cornea puncture properties of HA-MN patches, the corneas were isolated and fastened on a customized foam cushion. The HA-MN patches were fixed onto a cylindrical probe and were approached vertically to the cornea at a speed of 0.1 mm/s. The stress changes in a compression displacement of 0–1.2 mm were recorded. The *in vivo* cornea insertion performance of the HA-MN patches was evaluated by manually pressing the HA-MN patches on the cornea of the experimental animals for 60 s. Afterward, the corneas were observed under a slit lamp under cobalt blue light. After sacrificing the experimental animals, the corneas were extracted and subjected to histological examination.

2.5. Assessment of the HA distribution in cornea

To understand the *in vivo* stability of HA-MN patches in tears, the HA-MN patches were pressed onto the cornea of rats for 15, 30, and 60 s. The morphology changes of HA-MN patches were examined by a stereo-

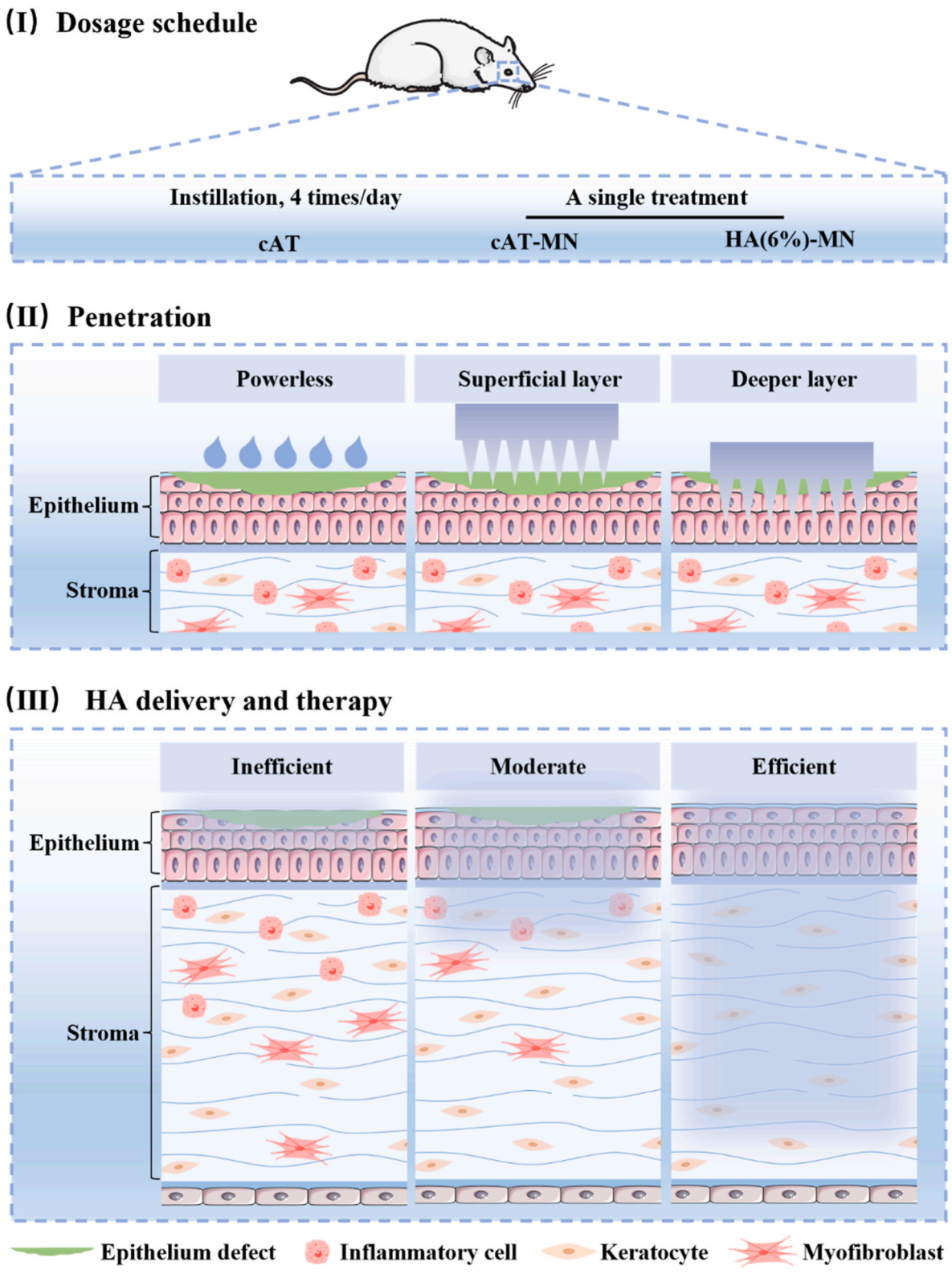

Fig. 1. Schematic illustration of HA-MN patches or -eye drop dosage for treating BAC-induced cornea damages. (I) The therapeutic dosage and administration of HA: cAT instillation (4 times/day for 10 consecutive days); cAT-MN patches insertion (single treatment in the first day); HA(6 %)-MN patches insertion (single treatment in the first day). (II) HA(6 %)-MN patches exhibited a glorious ability in corneal penetration. (III) A single administration of HA(6 %)-MN patches highlights an excellent therapeutic capacity in inhibition of BAC-induced corneal inflammation and stromal scarring, due to the efficient delivery of HA for the ocular surface.

optical microscope (SZ680, Optec, China). To visualize HA distribution in the cornea after HA-MN patches planting, the HA was labeled with Cy5.5 near-infrared fluorescent probe by grafting Cy5.5 onto HA according to the previous method [3], with minor modification. Briefly, HA was mixed with Cy5.5 amine for final mole ratios COOH in HA and NH_2 in Cy5.5 of 50/1. The reaction was initiated by adding EDC and NHS at room temperature for 24 h. The uncoupled Cy5.5 and any other contaminants were removed through dialysis. The sample was freeze-dried to obtain Cy5.5-grafted HA ($HA_{Cy5.5}$) powder. The $HA_{Cy5.5}$ instead of HA was used to fabricate the $HA_{Cy5.5}$(0.1 %) eye drop, $HA_{Cy5.5}$(0.1 %)-MN, and $HA_{Cy5.5}$(6 %)-MN patches. To understand the enhancement of HA retention in the cornea, the $HA_{Cy5.5}$(0.1 %)-MN (insertion), $HA_{Cy5.5}$(6 %)-MN (insertion), and $HA_{Cy5.5}$(0.1 %) eye drop (instillation) were *in vivo* administrated, respectively. After treatment, the distribution of $HA_{Cy5.5}$ in cornea was traced and compared in time course (0, 5, 10, 15, 20, 25, 30 min) with an *in vivo* fluorescence imaging system (IVIS, Spectrum, Perkin Elmer) under excitation and emission wavelength at 675 and 720 nm, respectively. The fluorescence intensity was quantitatively analyzed by measuring the average radiant efficiency (photons sec^{-1} cm^{-2} $sr^{-1}\mu W^{-1}$) in regions of interest (ROI). To further understand the improvement of stroma available for HA with MN-dosing, the rats were treated with corresponding dosing for 10 min, and then the corneas were extracted and laid flat on a slide. The fluorescence images were recorded under a confocal microscope using z-axis scanning (Zeiss LSM 880) at a step of 10 μm.

2.6. Biosafety evaluation of HA-MN patches

To understand the biosafety of MN patch insertion, the healthy animals were treated with these HA-MN patches. The level of corneal opacification, conjunctival hyperemia, and corneal neovascularization was evaluated at Pre (before MN-insertion), and 0 (just after MN-insertion), 6, 24, 48, and 72 h post-insertion. The corneal defection profile after MN administration was evaluated using a slit lamp using the above-mentioned method. The intraocular pressure changes before and after MN insertion were traced using a Schiotz tonometer (TV01, Icare, Finland). HCECs were used for the evaluation of cellular biosafety of HA-MN patches. HCECs were cultured in DMEM-F12 (Gibco) supplemented with 10 % FBS (Gibco), 5 μg/mL insulin (Gibco), 0.1 ng/mL EGF (Sigma-Aldrich), and 1 % penicillin/streptomycin solution (PH1513, Phygene, USA) at 37 °C in an incubator saturated with 5 % CO_2 and 95 % humidity. A density of 8×10^3 cells/100 μL HCECs were seeded in 96-well plates with four replicate wells per group. At 24 h after treatment with various concentrations of HA(6 %)-MN solution (contains HA and PVA dissolved in culture medium), 10 μL of CCK-8 reagent (Dojindo, Laboratories, Kumamoto, Japan) was added to each well. The optical density of each well was measured at 450 nm using an M5 SpectraMax® microplate reader (Molecular Devices, CA) after incubation for 2 h in the incubator.

2.7. Assessment of ocular surface repair efficacy

The animal model of BAC-induced ocular surface damage was constructed by instilling 0.3 % BAC (20 μL) twice per day for 10 consecutive days. To understand the therapy effects of different HA formulas, the modeling animals were treated with: 1) commercial artificial tears (cAT, contains 0.1 % HA) instillation (5 μL, 4 times/day for 10 consecutive days), 2) cAT-MN insertion (a single treatment), 3) HA(6 %)-MN insertion (a single treatment). The animals without BAC treatment were set as the healthy control. The level of corneal edema, conjunctival congestion, and corneal neovascularization were evaluated using a slit lamp under bright light at 0, 5, and 10 days after BAC treatment. Any corneal defects caused by BAC exposure were examined and scored by a skilled doctor under a slit lamp with cobalt blue light after fluorescein sodium staining.

2.8. Immunofluorescence staining and histological assay

The corneas were fixed, dehydrated, frozen, and sectioned into 10-μm-thick slices using a Cryostat (HM505E, Microm, Germany). The slices were then incubated with 0.3 % Triton X-100 and 10 % goat serum. Subsequently, the sections were incubated with the primary antibody at 4 °C overnight and secondary antibodies at room temperature for 2 h in sequence. The primary antibodies, rabbit anti-IL-1β (1/200, Proteintech, 26048-1-AP), mouse anti-8-OHdG (1/200, Abcam, ab62623), rabbit anti-NLRP3 (1/200, Proteintech, 19771-1-AP), rabbit anti-α-SMA (1/200, Abcam, ab5694), and rabbit anti-TNF-α (1/200, Proteintech, 17590-1-AP) were employed in these experiments. Immunofluorescence images were recorded under a confocal microscope (Zeiss LSM 880, Germany) and quantified using the ImageJ software. The sections were further subjected to histological assay with the following process: incubating with hematoxylin buffer and eosin solution, rehydrating in alcohol gradients, and mounted on a slide. Histological images were observed under a microscope (DM4 B, Leica, Germany). PAS staining was performed using a kit (PH1144, Phygene, China). Briefly, the corneas were fixed, dehydrated, embedded in paraffin, and sectioned into 10-μm-thick slices by a Microtome (RM2125 RTS, Leica, Germany). The sections were incubated with a periodic acid solution and Schiff reagent in sequence. Images were recorded under a microscope (DM4 B, Leica, Germany).

2.9. Statistical analysis

The data are presented as means ± S.D. Statistical analyses were performed using one-way or two-way analysis of variance (ANOVA). Differences of *, $p < 0.05$; **, $p < 0.01$; ***, $p < 0.001$; ****, $p < 0.0001$ were considered statistically significant.

3. Results

3.1. Fabrication and characterization of HA-MN patches

The cornea of a rat has a radius of 2970 ± 2 μm. The thickness of the cornea of the rat is 198.0 ± 9.9 μm with epithelium and stromal thickness of 38.4 ± 1.2 μm and 83.3 ± 9.6 μm, respectively [27,28]. In line with the parameter of rat cornea, squared MN patches with 5 × 5 mm in length were designed and prepared (Fig. S1). The MN patches possessed a 7 × 7 conical microneedles (500 μm in height and 400 μm in base diameter) array distributed eventually. We first tried to fabricate the cAT-MN by casting artificial tears (containing 0.1 % HA) directly. However, it failed to de-molding (Fig. S2). To facilitate cAT-MN preparation, PVA was added as an excipient to commercial artificial tears. With the addition of PVA to the pre-casting solution, intact HA-MN patches with uniform morphology were obtained (Fig. 2A–B, S3, and Tables S1–2). These HA-MN patches were foldable, twistable, and stretchable, indicating an advantage in fitting the ocular surface tissue that has a certain degree of curvature (Fig. 2C–D, and S4). Under compression stress, HA-MN patches have a significantly stronger mechanical performance than the cAT-MN patches, probably attributed to adding the PVA into the MN patches (Fig. 2E). Increasing HA content in HA-MN patches, which lowered the PVA content, changed compression stress from 0.32 ± 0.02 N per needle (HA (0 %)-MN) to 0.13 ± 0.01 N per needle (HA (10 %)-MN).

3.2. Corneal puncture properties of HA-MN patches

The *in vivo* corneal puncture ability of the HA-MN patches was tested on rats. As shown in Fig. 3A, an inerratic dot matrix-like fluorescein staining was observed on the ocular surface after being pressed with HA-MN patches, indicating successful penetration of the corneal epithelium. The size of the staining dot in the HA(6 %)-MN group was larger than that in the cAT-MN group. This suggested that HA(6 %)-MN possessed

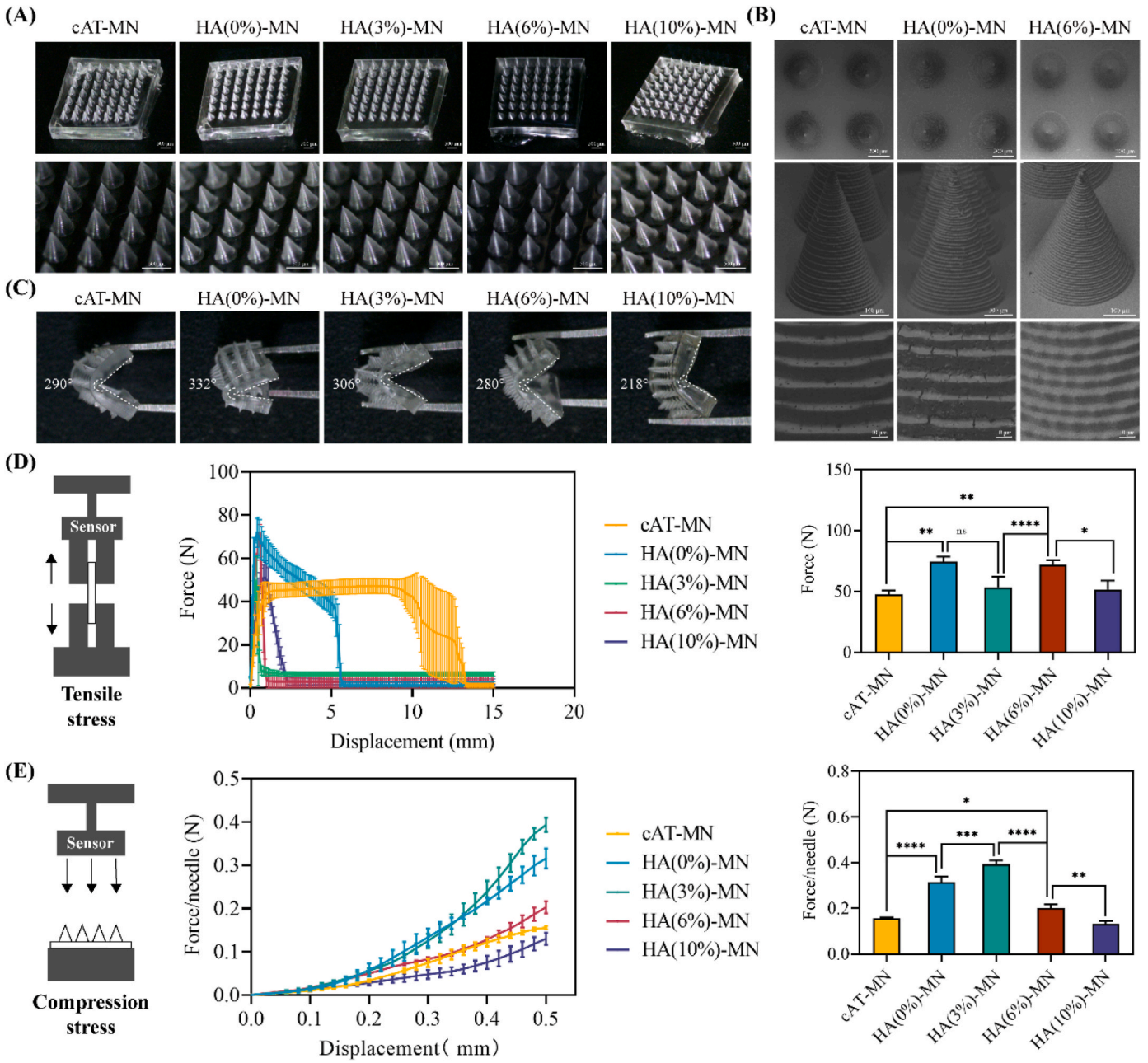

Fig. 2. Fabrication and characterization of HA-MN patches. (A) Representative bright-field microscopy images of MN patches. Scale bars = 500 μm. (B) Representative SEM images of MN patches. Scale bars = 200 μm (up), 100 μm (center), and 10 μm (down), respectively. (C) The flexibility test of the MN patches. (D) Schematic illustration (left), force-displacement profiles (middle), and average maximum forces (right) of MN patches during application of tensile forces. (n = 3; *p < 0.05, **p < 0.01). (E) Schematic illustration (left), force-displacement profiles (middle), and average maximum forces (right) of MN patches during application of compressive forces. (n = 3; *p < 0.05, **p < 0.01, ***p < 0.001, ****p < 0.0001).

higher corneal penetration ability than cAT-MN (conical needle, the radius was gradually increased from tip to the bottom). This could be further confirmed by H&E examination (Fig. 3B). The MN containing Cy5.5 labeled HA was then administrated. Results showed that this MN can effectively deliver the HA to corneal stroma (Fig. 3C–D), indicating it can break the corneal epithelium and the pre-corneal barrier. To figure out how much of the force is needed for corneal puncture, the *ex vivo* cornea penetration experiment was performed (Fig. 3E). The force changes during the penetration process were detected and recorded using a texture analyzer. An obvious discontinuity in the force-displacement curve was observed in HA(6 %)-MN group at a displacement distance of 0.87 with a force of 0.0020 ± 0.0004 N per needle. Results suggested that around 0.0020 N per needle of the force was needed for corneal epithelium puncture when HA(6 %)-MN was administrated on rat.

3.3. MN patches enhance HA-delivery to corneal stroma

The stability of HA-MN patches in tears, representing the time window for operation (tissue insertion), is the key indicator of the MN patches for cornea insertion. The *in vivo* stability of MN patches in tears was investigated by pressing the HA-MN patches onto the corneas of experimental animals for 15, 30, and 60 s. The morphology changes of HA-MN patches were monitored under a microscope after being removed away from the eye (Fig. 4A). As shown in Fig. 4B, the cAT-MN was tear-stable in 60 s of immerging. The HA(6 %)-MN patches

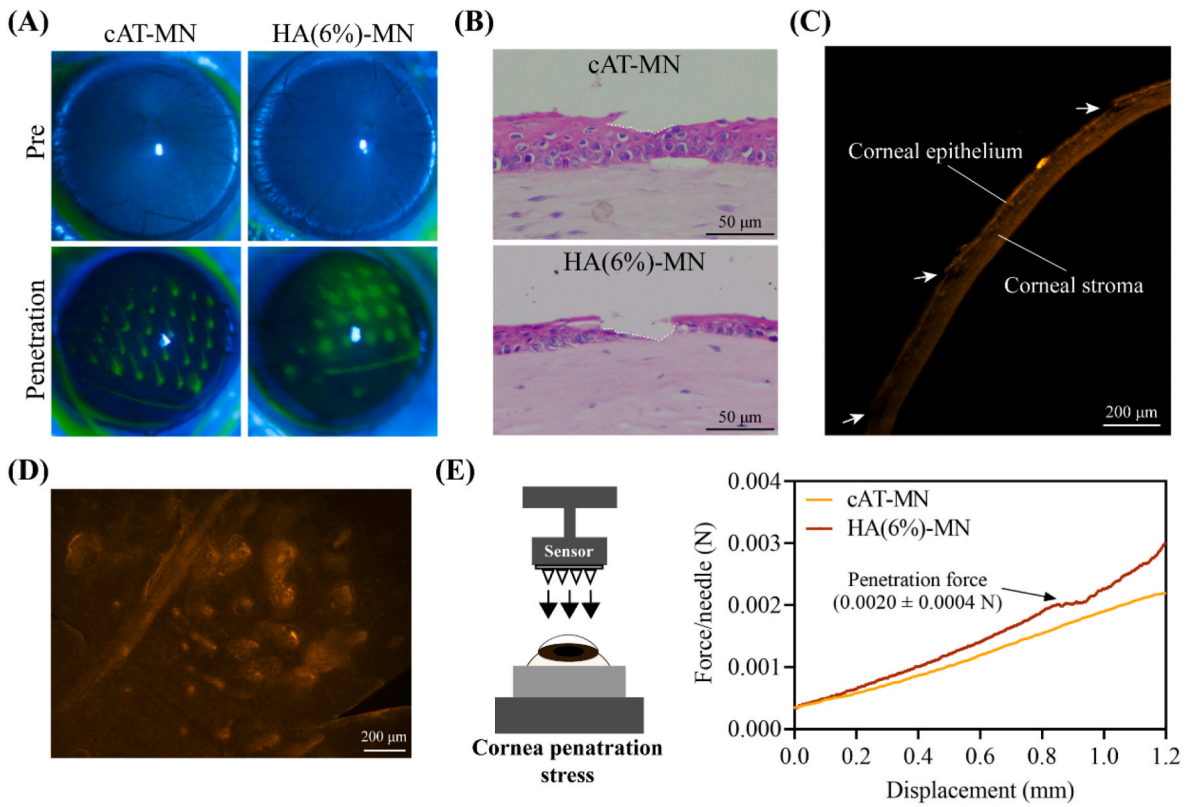

Fig. 3. Corneal penetration of HA-MN patches. (A) Photographs of corneal fluorescein staining by cobalt blue light under a slit lamp before and after penetration of HA-MN patches into the rat cornea. (B) The representative histological changes of rat cornea after HA-MN patches penetration. Scale bar, 50 μm. (C–D) The representative fluorescence images of rat corneal section (C) or surface (D) after treatment with Cy5.5 mixed HA(6 %)-MN patches. Scale bar, 200 μm. (E) Schematic illustration (left) and the averaged penetration force (right) of HA-MN patches into the rat cornea.

exhibited less tear-stable than cAT-MN patches. The *in vivo* HA-retention on the ocular surface after topical instillation (HA(0.1 %) eye drop) and MN patches insertion (HA(0.1 %)-MN patches and HA(6 %)-MN patches) were compared. The Cy5.5 labeled HA was employed in these experiments. The retention of HA on the ocular surface was traced (Fig. 4C–D, and S5). After $HA_{Cy5.5}$(0.1 %) eye drop instillation, a slight fluorescence signal can be observed in the first 15 min of administration. While negligible fluorescence signal was observed after 20 min post-instillation. Compared to $HA_{Cy5.5}$(0.1 %) eye drop instillation, an obviously higher fluorescence intensity was detected in the ocular surface, when $HA_{Cy5.5}$(0.1 %)-MN patches were administrated (insertion). Further enhancement in fluorescence intensity in the ocular surface was observed with an increase in the $HA_{Cy5.5}$ content in $HA_{Cy5.5}$(6 %)-MN patches. To understand the distribution of HA in corneal stroma, corneas from the experimental animals receiving various treatments were extracted and fixed onto a slide and observed under a confocal scanning light microscopy (CSLM) under a z-axis scanning model (Fig. 4E). As shown in Fig. 4F, a nearly undetectable level of $HA_{Cy5.5}$ can be observed in the cornea from surface to inside (0–110 μm), suggesting limited stroma available for HA after topical instillation ($HA_{Cy5.5}$(0.1 %)). With $HA_{Cy5.5}$(0.1 %)-MN patches insertion, the tensity $HA_{Cy5.5}$ signal was detected in the superficial layer (0–60 μm), while the signal gradually faded in the cornea in the deep layer (70–110 μm), indicating the limited ability in HA-delivery. While, the $HA_{Cy5.5}$(6 %)-MN patches could significantly improve HA-delivery into the stroma, achieving a depth of 110 μm into the cornea, exhibiting superior HA-delivery efficiency to the corneal stroma.

3.4. Biosafety of HA-MN patches

The *in vivo* biosafety of HA-MN patches was examined in rats for 72 consecutive hours. As shown in Fig. 5A, both cAT-MN and HA(6 %)-MN patches caused no significant changes to corneal opacification, conjunctival hyperemia, and corneal neovascularization. However, at the moment of piercing, MN patches both caused an obvious array of point-like fluorescein staining, indicative of corneal epithelium defect (Fig. 5B). While the fluorescein staining obviously decreased after 6 h and nearly disappeared after 24 h. These suggested the deficiency of corneal epithelium caused by HA-MN patches could be self-healing within a short time. In addition, the intraocular pressure (IOP) was monitored comprehensively. As shown in Fig. 5C, the intraocular pressure was decreased at the moment of puncture (Penetration) both after cAT-MN (3.44 ± 0.53 mmHg) and HA(6 %)-MN (3.89 ± 1.36 mmHg) patches treatment, comparing to the healthy rat with IOP of 9.11 ± 1.27 mmHg and 8.56 ± 0.73 mmHg. The IOP then rose rapidly within 5 min with an IOP of 7.44 ± 1.74 mmHg (cAT-MN group) and 6.67 ± 2.5 mmHg (HA(6 %)-MN group), and recovered to a healthy level with an IOP of 10.11 ± 1.05 mmHg (cAT-MN group) and 8.67 ± 2.18 mmHg (HA(6 %)-MN group) within 10 min, respectively. The valuable biosafety of HA-MN solution was further confirmed in human corneal epithelial cells (HCECs) (Fig. 5D). These results highlight the good biosafety of HA-MN patches for the ocular surface.

3.5. HA-MN patches alleviate BAC-induced DED syndrome

Repeating exposure of ocular surface to BAC can damage both the superficial tissue (e.g., corneal epithelial cell apoptosis (Fig. S6) and conjunctival goblet cells loss) [20,21] and the inside structures (e.g., lymphocyte/inflammatory cell infiltration to the stroma, upregulation of inflammatory factors, corneal neovascularization, stromal scaring) [22–24]. In this study, the therapeutic effects of cAT eye drops (instillation) were compared to its MN dose form (insertion) (Fig. 6A). The cAT

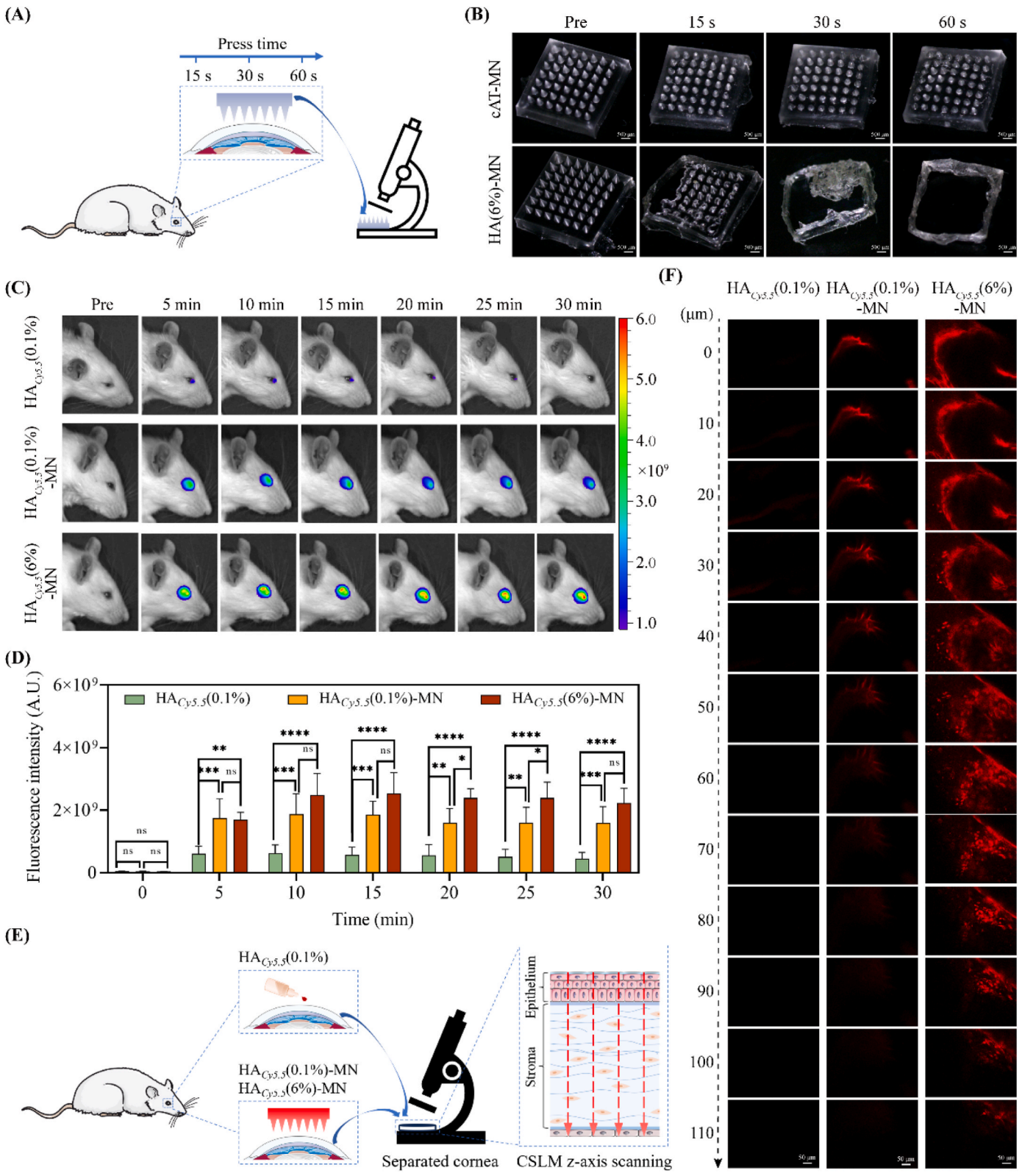

Fig. 4. MN patches enhance HA delivery for corneal stroma. (A–B) Schematic illustration (A) and representative bright-field microscopy images (B) of HA-MN patches at 15, 30, and 60 s post-administration. Scale bars, 500 μm. (C–D) Fluorescence intensity (C) and quantitation (D) of Cy5.5-grafted HA (HA$_{Cy5.5}$) in rat eye after indicated treatments. (n = 4; *p < 0.05, **p < 0.01, ***p < 0.001, ****p < 0.0001). (E–F) Schematic illustration (E) and representative fluorescence images (F) of different layer depths distribution of HA$_{Cy5.5}$ within rat cornea after indicated treatments, examined through z-axis scanning by confocal scanning light microscopy (CSLM). Scale bar, 50 μm.

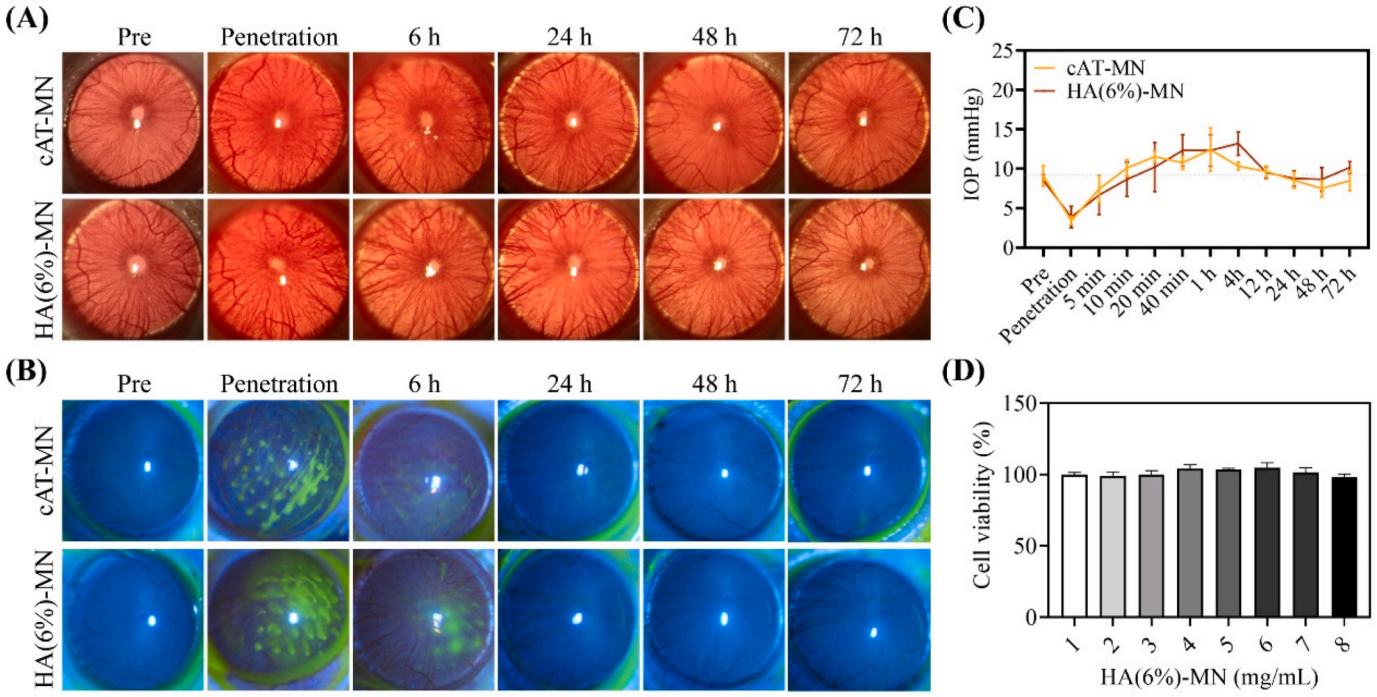

Fig. 5. Biosafety of HA-MN patches. (A–B) Photographs of cornea clinical signs by bright light (A) and cobalt blue light (B) under a slit lamp with HA-MN patches administrations for 72 consecutive hours. (C) Intraocular pressure of rats treated with HA-MN patches was recorded for 72 consecutive hours (n = 6). (D) Cellular biosafety of HA(6 %)-MN solution with various concentrations in HCECs for 24 h (n = 4).

instillation was administrated 4 times/day for 10 days. The cAT-MN insertion was conducted only once at the initiated time point during the experiment period (10 days). As shown in Fig. 6B–F, repeating exposure to BAC for 5 days caused large-scale corneal epithelium defect, corneal edema, and ocular surface inflammation (NS group). Compared to the situation for 5 days of BAC exposure, the corneal epithelium defect level has reduced in 10 days of BAC exposure (still significantly higher than the healthy control), probably due to the powerful self-healing nature of the corneal epithelium [29]. However, the situation for the corneal edema and ocular surface inflammation deteriorated steadily within the elongation of the BAC exposure period. Topical instilling of cAT (1 or 4 times/day) or HA(0.1 %) liquid (4 times/day) (Figures S7, 5B-F, and S8) did not exhibit the corneal protection effects against these heavy damages. With the aid of microneedle, both the cAT-MN patches and HA(0.1 %)-MN patches (Fig. S9) significantly prevented the progress of corneal damages in the first 5 days of BAC exposure. However, it showed limited effects at the 10 days of BAC exposure, accounting for running out of the supplied HA in MN patches. Additionally, the HA(0 %) -MN patches (without HA) did not show obvious corneal protection effects against BAC-induced damage, suggesting that the HA is the protection factor within those MN patches (Fig. S10). To expand the therapy effects, the HA(6 %)-MN patches were employed to prevent severe BAC-induced corneal damages. Compared to the effects of cAT-MN patches, a single administration of HA(6 %)-MN patches exerted a 10-day DED syndrome therapeutic effects against BAC exposure, which could be attributed to adding stroma-available for HA both by increasing the amount of HA delivered and enhancing corneal permeation (Figs. 3 and 4). Besides the harm to tissues, BAC exposure could also impair the physiological activity of ocular tissues (e.g. tear production), which is one of the clinical manifestations of DED syndrome [30]. As shown in Fig. S11, a 10-day BAC exposure significantly reduced the tear secretion. While HA(6 %)-MN patches treatment could restore tear volume to a healthy level. These results manifested that HA (6 %)-MN patches treatment could recover the level of BAC-induced DED syndrome to healthy control, promising a wide clinical use in ophthalmology.

3.6. HA -MN patches prevent BAC-induced histological changes of ocular surface structure

To further understand the corneal protection effects of those treatments, the tissues from the animals receiving various treatments were extracted, sectioned, and further subjected to histological analysis. The corneal epithelium consists of 6–8 layers of tightly aligned cells; while the corneal stroma is a lamellar structure composed of the precise alignment of collagen and keratocytes which make up ~90 % of the cornea and is essential for the unique properties and function of the cornea (e.g. transparency, photorefraction, avascularity, mechanical properties) [31]. Any insult to the cornea could cause pathological changes (e.g. corneal swelling, loss of corneal transparency, inflammatory cell infiltration, epithelium defection) in the cornea. With BAC exposure for 5 days, there were no significant changes in the thickening of the epithelium and the stroma can be observed. A slight increase in inflammatory cell density in the stroma was observed in the NS group (Fig. 7A). The BAC has caused a substantial inflammatory cell infiltration to the stroma and the stroma swelling as well, in a 10-day exposure. Topical instillation of cAT exerted some inhibiting effects on such changes when compared to the NS group; while it had a significantly higher corneal injuring index (e.g. inflammatory cell infiltration, stroma swelling), compared to the group of health control. A single administration (insertion) of cAT-MN patches exhibited more efficiency in inhibiting corneal injury than the cAT treatment; however, the symptoms could not recover to a healthy level. Among these treatments, HA (6 %)-MN patches could restore the cornea tissue to a healthy structure, exerting the best therapeutic effect against BAC-induced corneal injury.

Besides the cells in the cornea, the conjunctival goblet cells (GCs) which support the production and renewal of mucin (at the innermost of tear film) are essential for the physiological homeostasis of ocular surface [32]. As depicted in Fig. 7E and F, repeating BAC exposure for 5 days exhibited a slight decrease in the density of goblet cells and atrophy of the GCs (no significant difference). These pathologic conditions tend to deteriorate after 10-day BAC clonic exposure (with a significant difference). The cAT eye drop could not rescue the goblet cells; while the

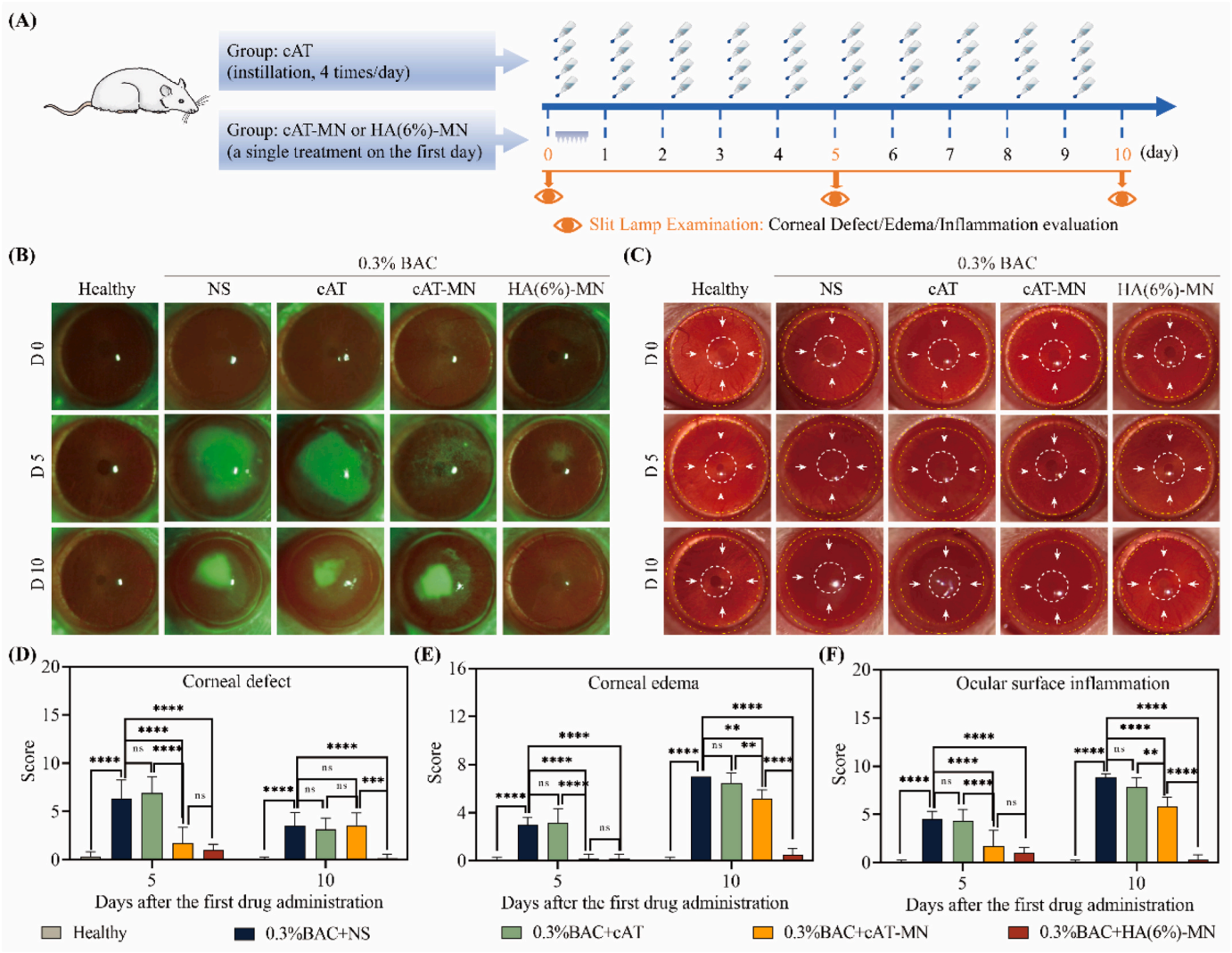

Fig. 6. HA-MN patches alleviate BAC-induced DED syndrome. (A) Schematic illustration of different HA dosage administrations in BAC-treatment rats. (B–C) Photographs of cornea clinical signs by cobalt blue light (B) and bright light (C) under a slit lamp with different administrations after 0, 5, and 10 days. Yellow dashed curve: conjunctival hyperemia. White arrow and dashed circle: opacification of the peripheral and central cornea, respectively. (D–F) Corneal defect (D), corneal edema (E), and ocular surface inflammation (F) evaluation of the rats treated with different therapies after 5 and 10 days (n = 6; **p < 0.01, ***p < 0.001, ****p < 0.0001).

cAT-MN exhibited a certain protective ability on goblet cells. However, HA(6 %)-MN patches exhibited a desirable capacity to prevent BAC-induced goblet cell loss, which showed no significant difference from the levels in the healthy group. These results suggested the potential of HA(6 %)-MN patches to curb the BAC-induced ocular surface damages.

3.7. HA-MN patches inhibit corneal inflammation and stromal scarring

It is reported that BAC could up-regulate the expression of the inflammation factor IL-1β and inflammasome NLRP3 in HECEs [6], which was also verified in this study (Fig. S12). To further investigate the effects of HA-MN patches on reducing the inflammation within the cornea, we examined IL-1β expression by immunofluorescent staining. As shown in Fig. 8A–C, repeated exposure to BAC significantly increased the IL-1β level both in the corneal epithelium layer and stroma layer. Instilling cAT (4 times/day) could not inhibit up-regulation of IL-1β level under BAC in 5-day post-administration. The IL-1β level (both in corneal epithelium and stroma) was recovered to a certain extent in a 10-day administration (cAT instillation, 4 times/day), whereas higher than that in healthy corneas. A single administration of cAT-MN could significantly reduce the IL-1β level both in the corneal epithelium layer and stroma layer, whereas still significantly higher than that in healthy control. Administration of the HA(6 %)-MN patches recovered the IL-1β to a healthy level both in the corneal epithelium layer and stroma layer. Our previous studies suggested that the signaling axis mitochondria DNA oxidation-NLRP3 inflammasome activation-IL-1β maturing and releasing were involved in BAC-induced corneal damage [5,6]. Thus, we further compared the level of mitochondria DNA oxidation and NLRP3 inflammasome in corneas. Repeated exposure to BAC for 5 days significantly increased the 8-OHdG level (biomarker of DNA oxidation) in the corneal epithelium, whereas not in the stromal layer (Fig. 8D–F). The 8-OHdG level in the stroma was significantly enhanced after prolonging the period of BAC exposure (10 days). Frequency instillation of cAT could not inhibit the elevation of 8-OHdG levels both in epithelium and stroma. While a single administration of cAT-MN patches could down-regulate 8-OHdG level in epithelium other than the level in the stroma. The HA(6 %)-MN patches could restore the 8-OHdG level to the healthy control, indicating the valuable capacity of HA(6 %)-MN patches in the prevention of mitochondria DNA oxidation. Repeated exposure to BAC did not change the NLRP3 expression both in the corneal epithelium and the stroma after 5 days post-administration

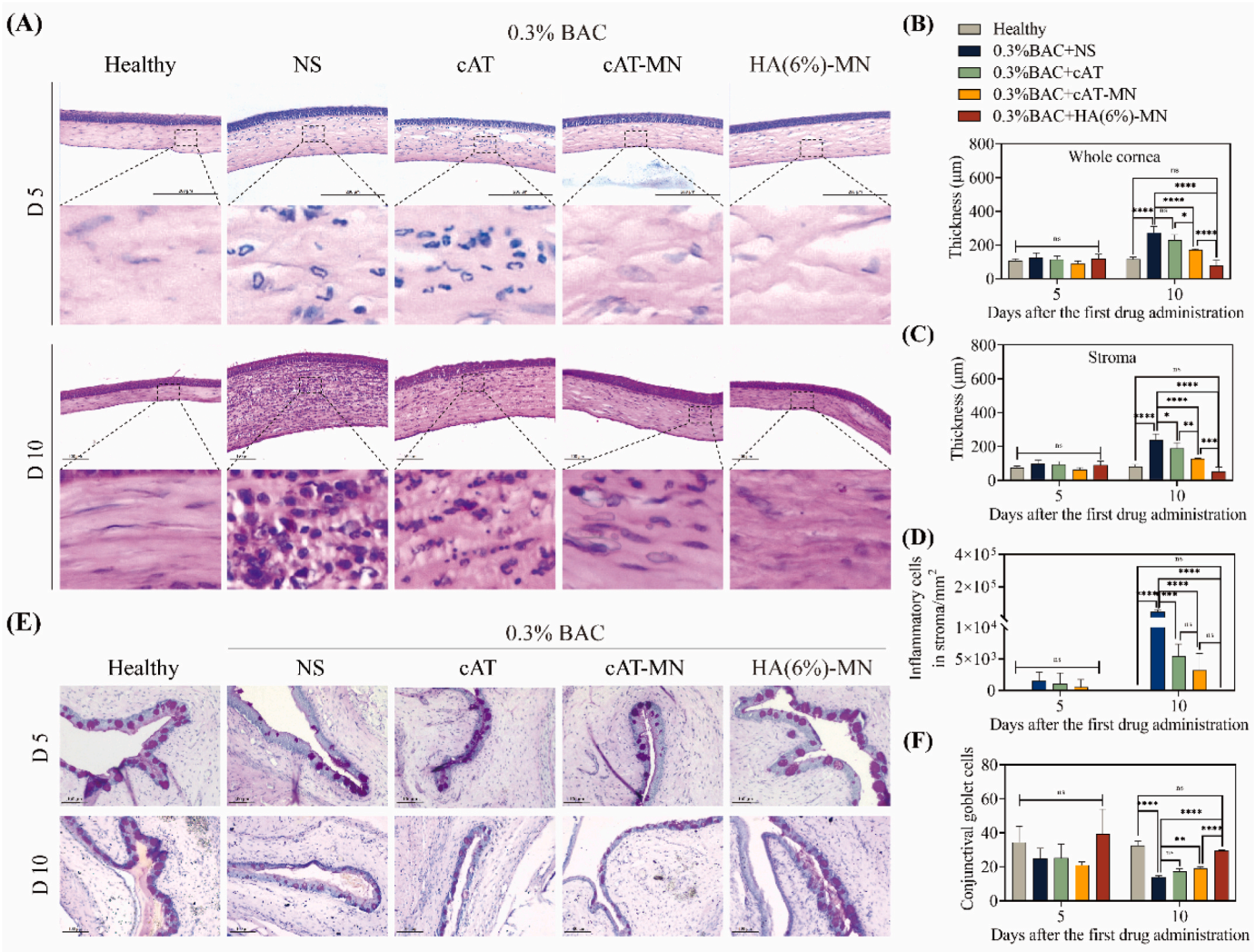

Fig. 7. HA-MN patches prevent BAC-induced histological changes of ocular surface structure. (A) Typical hematoxylin and eosin (H&E) staining of the rat cornea on day 5 and day 10 post different administrations. Scale bars = 200 μm (D 5 groups) or 100 μm (D 10 groups). (B–E) Quantitative analysis of whole corneal thickness (B), corneal stroma thickness (C), and inflammatory cells in stroma (D) of the rats treated with different therapies after 5, and 10 days (n = 3 to 6; *p < 0.05, **p < 0.01, ***p < 0.001, ****p < 0.0001). (E–F) Representative images (E) and quantitative analysis (F) of PAS staining of conjunctival goblet cells of the rats treated with different therapies after 5 and 10 days (n = 3 to 6; **p < 0.01, ****p < 0.0001).

(Fig. 8G–I). With a 10-days of BAC exposure, NLPR3 expression was significantly enhanced within corneal stroma other than in the epithelium. Installation of cAT and insertion of cAT-MN patches showed a comparable level of NLPR3 expression. HA(6 %)-MN patches nearly restored the NLRP3 expression of corneal stroma to a healthy level. These results demonstrated that HA(6 %)-MN patches could block the ox-mtDNA/NLRP3/IL-1β pathway, resulting in a favorable protective capacity for cornea against BAC.

Accumulation of inflammation within corneal stroma is seen to contribute to stromal scarring, which is a pivotal therapeutic target for restoring corneal transparency [33]. We evaluated the corneal scaring level using immunofluorescent staining analysis for α-SMA. As shown, BAC could significantly trans-differentiate the quiescent stromal keratocytes (α-SMA-negative) into metabolically active corneal myofibroblasts (α-SMA-positive), which indicated the happening of corneal scarring (Fig. 8J–K). cAT or cAT-MN patches treatment could significantly reduce α-SMA-positive myofibroblasts, while HA(6 %)-MN patch exhibited the best repressive effects with invisible myofibroblasts similar to the healthy stroma.

4. Discussion

Trauma to the cornea triggers a series of events that even could lead to blindness, is occurs from a wide range of environmental factors, including a wide use of harmful preservatives such as BAC in ophthalmological solutions [8,16]. Repeated applications of BAC could insult deeper tissue of the cornea and induce lymphocyte infiltration and upregulation of inflammatory factors, leading to corneal scarring and sight-threatening even blinding [22–24,34]. Topical administration of steroids, doxycycline, immunomodulators, etc, are generally adopted clinically to manage corneal stroma damage. However, repeating administration of these agents caused serious side effects (e.g., glaucoma, cataracts, delayed wound healing) [35]. Keratoplasty is the only option for curing severe stroma damage to restore vision [36,37]. Nonetheless, it is limited by the lack of transplantable materials [38]. It is of great significance to develop a new treatment with high biocompatibility for both corneal superficial layer (epithelium) and deeper layer (stroma) repair for the BAC-induced cornea damage.

HA is a natural biopolymer in cell-matrix (throughout the human body) with super high biocompatibility [39]. Rare side effects of HA have been documented in the literature. Besides, it has several favorable

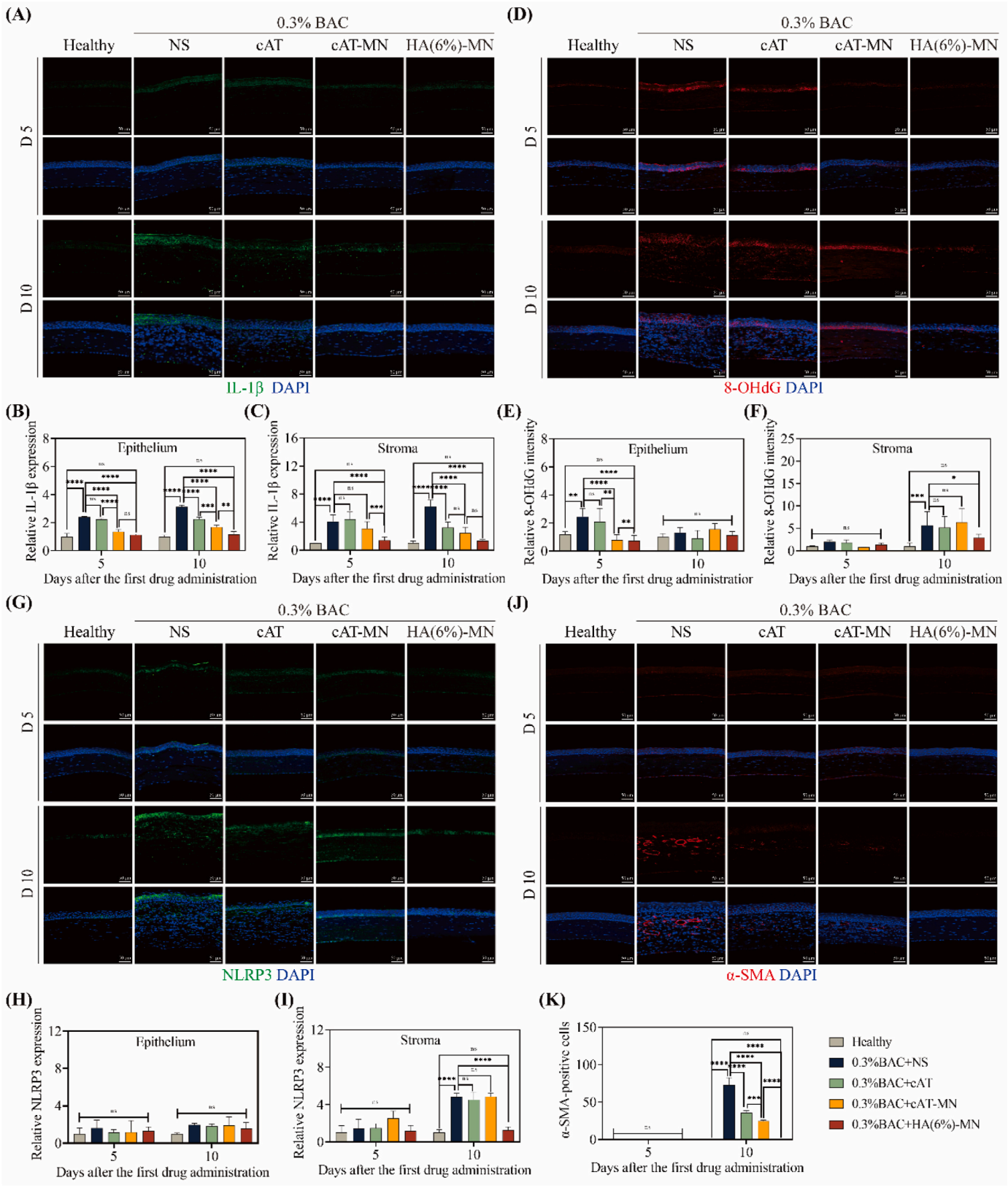

Fig. 8. HA-MN patches inhibit BAC-induced corneal inflammation and stromal scarring. Representative immunofluorescence staining and quantitative analysis of the rat cornea for IL-1β (A–C), 8-OHdG (D–F), NLRP3 (G–I), and α-SMA (J–K) treated with different therapies after 5, and 10 days. Scale bars, 50 μm. (n = 3 to 9; *p < 0.05, **p < 0.01, ***p < 0.001, ****p < 0.0001).

bioactivities (e.g. antioxidant, immune regulation, anti-inflammatory) [7,39,40], making it a wide biomedical application. HA has been engineered to form diverse device/drug delivery systems (e.g. nanofibers, hydrogels, micro/nano gels, and scaffolds) to facilitate delivering of a diverse of therapeutic agents (e.g. anti-inflammatory drugs, genes, and cell therapies) via different administration routes [39]. Moreover, It has been favorably employed to fabricate dissolvable MNs to overcome several onsite biological barriers (e.g. derma, ocular) [41,42]. Collectively, HA is widely used as a drug delivery system as described above. The intrinsic properties of HA, encompassing both its polymeric architecture and inherent biological activity, render it particularly advantageous for therapeutic applications. Notably, Li et al. have designed a drug-free HA nanoparticle and it exhibited significant therapeutic ability in osteoarthritis treatment by targeting CD44 [43]. Furthermore, Yao et al. have developed a novel drug-free non-crosslinked chitosan/HA hybrid hydrogel via electrostatic interactions, which exhibited remarkable wound healing properties [44]. For ophthalmological applications, a drug-free HA hydrogel engineered by Jeremy Chae et al. is capable of sustaining IOP reduction for up to four months following suprachoroidal administration [45]. In this study, we innovatively propose to prepare a new drug-free HA microneedle patch for corneal disorder management. This HA-MN patch demonstrates great biocompatibility and significant anti-inflammatory and anti-scarring efficacy for benzalkonium chloride-induced corneal disorders (Figs. 6–8). The drug-free nature of this single-dose therapeutic approach eliminates the need for daily patient compliance, presenting a promising alternative for the treatment of corneal pathologies. The integration of intrinsic biological properties of HA with advanced drug delivery technology positions this innovation as a potentially transformative therapeutic modality in ophthalmology.

Due to its good biocompatibility and versatile bioactivities, HA is a favorable material in commercial artificial tears to relieve mild disorders in the ocular surface. However, topical administration of these HA solutions (artificial tears) showed limited therapy effectiveness on heavy disorders that have further involved corneal stroma damages, due to its low stroma-available resulting from the barrier of corneal epithelium. HA-delivery to the deeper layer of the cornea with MN would be an advanced strategy since the existing treatments (e.g., topical instillation, stromal injections) are associated with one or some of the following shortcomings: limited permeability, low bioavailability, high risk of infections, and poor patient compliance [46,47]. When topical administrated, a rate of more than 90 % of HA is removed from the ocular surface within 30 min, and the retentate (HA) showed extreme hardness to cross the epithelium of the cornea [48–50]. In our study, the HA-based artificial commercial tear liquid (cAT, which contains 0.1 % of HA) was fabricated into dissolvable, flexible, disposable, and drug-free MN patches. Compared to other types of MNs such as solid MNs, coated MNs, or hollow MNs, dissolving MNs can degrade in the inserted tissue thereby releasing the encapsulated agents in a sustained manner, while also overcoming the penetration barriers due to specific design [51]. Our desiged dissolving cAT-MN (microneedle dosage form of commercial artificial tear) has a valuable ability to penetrate the epithelium barrier in the cornea (Fig. 3). Compared to eye drop formulation (cAT), the cAT-MN obviously elevated the HA content in the stroma (Figs. 3 and 4), hence has a better therapy effect on BAC-induced corneal injury. To expand its therapy effects, MN patches containing 6 % HA were prepared, which could recover the BAC-induced corneal damage (no significant difference with the healthy control). By enhancement of the bioavailability of HA, the frequency of medication was reduced. Single administration (in 10 days) of the HA-MN patches exhibited higher therapy effects than topical instilling of the commercial HA formula (4 times/day for 10 days). These HA-based drug-free MN exhibited valuable capacity in restoration of both corneal epithelium and stroma, due to the improved HA-delivery towards the superficial as well as the deeper layer of the cornea, hopefully a wide clinical use in ophthalmology. It will be of great significance to further explore the potential application of HA-MN patch in other causes of corneal damage, such as laser refractive surgeries, ocular infection, and ocular trauma, which cause significant corneal stroma scarring [52–54].

Besides enhancing the stroma available for HA, this HA-MN exerted a curing effect on BAC-induced corneal damage without the need for toxicity agents, which avoids those generally addressed side effects. As mentioned above, BAC could cause corneal epithelium defect, inflammatory cell infiltration, stromal edema, etc, which may sight-threatening even blinding. Clinically, steroidal anti-inflammatory agents such as dexamethasone, prednisolone, methylprednisolone, and fuorometholone etc, are commonly included in the therapeutic regimen [55]. However, repeated topical instillation of these agents results in a serial severe side effect; therein, bringing about a rise in intraocular pressure (IOP) is the most significant one [12,56]. By using MN technology, the HA instead of those toxicity agents was employed and exhibited powerful inhibition activity against BAC-induced corneal injury (both in the epithelium and stroma), highlighting the biosafety and effectiveness of this HA-based MN patch.

Though MN insertions are generally recognized as minimally invasive administration, it is necessary to evaluate the biosafety of MN insertion case by case. After insertion of the HA-based MN patches, a short-term corneal epithelium defect (<1 day) and transient (<10 min) decrease of IOP was observed (Fig. 5A–C). The recovery of the corneal defect was faster than previously reported MN patches (3 days) [15]. Transient fluctuation of IOP which has been usually observed after suprachoroidal space injection (~20 min) [57] and intravitreal injection (~15 min) [58], is considered no obvious risk for the eye. These indicated it is safe to use this MN for ocular surface medication.

5. Conclusion

In this study, a microneedle-dose form of commercial artificial tear (cAT-MN, containing 0.1 % of HA) was fabricated and characterized. These HA-MNs can override the on-site precorneal barrier and the corneal epithelium barrier, which increases the therapy effects on BAC-induced corneal injury and concurrently reduces the medication frequency. A single dose of cAT-MN (corneal insertion) exhibited significantly higher therapy effects than repeating instillation of cAT (4 times/day) against BAC-induced corneal injury (both in the epithelium and the stroma). To expand its therapy effects, MN patches containing 6 % HA were prepared, which could recover the BAC-induced corneal damage completely (no significant difference with the healthy control). In a mechanistic sense, these HA-based MNs prevented BAC-induced corneal injury (both in the epithelium and the stroma) by inhibition of ox-mtDNA/NLRP3/IL-1β pathway. This work presents a new form (or dose regimen) of HA-based commercial artificial tears to cure corneal stroma disorders which have expanded its indication, promising a wide clinical use in ophthalmology.

CRediT authorship contribution statement

Baoshan Huang: Writing – review & editing, Writing – original draft, Project administration, Methodology, Investigation, Funding acquisition, Formal analysis, Data curation, Conceptualization. **Rui Zeng:** Methodology, Investigation. **Xiao Liu:** Methodology, Investigation. **Lu Pan:** Methodology, Investigation. **Haitong Bai:** Investigation. **Jiachen Liao:** Investigation. **Wenkai Xu:** Investigation. **Hong Fu:** Investigation. **Kaihui Nan:** Writing – review & editing, Project administration, Funding acquisition, Data curation. **Sen Lin:** Writing – review & editing, Validation, Supervision, Resources, Project administration, Funding acquisition, Data curation, Conceptualization.

Declaration of competing interest

The authors declare that they have no known competing financial interests or personal relationships that could have appeared to influence the work reported in this paper.

Acknowledgments

This work was financially supported by the Basic Research Project of Wenzhou City (ZY2021018) and Zhejiang Provincial Natural Science Foundation of China (LY19H120002, LQ23H120002).

Appendix A. Supplementary data

Supplementary data to this article can be found online at https://doi.org/10.1016/j.mtbio.2025.101722.

Data availability

Data will be made available on request.

References

[1] D.A. Semp, D. Beeson, A.L. Sheppard, D. Dutta, J.S. Wolffsohn, Artificial tears: a systematic review, Clin. Optom. 20 (15) (2023) 9–27.
[2] M.J. Rah, A review of hyaluronan and its ophthalmic applications, Optometry 82 (1) (2011) 38–43.
[3] S. Lin, W. Gao, C. Zhu, Q. Lou, C. Ye, Y. Ren, R. Mehmood, B. Huang, K. Nan, Efficiently suppress of ferroptosis using deferoxamine nanoparticles as a new method for retinal ganglion cell protection after traumatic optic neuropathy, Biomater. Adv. 138 (2022) 212936.
[4] G. Agarwal, K.K. V, S.B. Prasad, A. Bhaduri, G. Jayaraman, Biosynthesis of hyaluronic acid polymer: dissecting the role of sub structural elements of hyaluronan synthase, Sci. Rep.-UK 9 (1) (2019) 12510.
[5] B. Huang, N. Zhang, X. Qiu, R. Zeng, S. Wang, M. Hua, Q. Li, K. Nan, S. Lin, Mitochondria-targeted SkQ1 nanoparticles for dry eye disease: inhibiting NLRP3 inflammasome activation by preventing mitochondrial DNA oxidation, J. Contr. Release 365 (2024) 1–15.
[6] Q. Lou, L. Pan, S. Xiang, Y. Li, J. Jin, J. Tan, B. Huang, K. Nan, S. Lin, Suppression of NLRP3/Caspase-1/GSDMD mediated corneal epithelium pyroptosis using melatonin-loaded liposomes to inhibit benzalkonium chloride-induced dry eye disease, Int. J. Nanomed. 18 (2023) 2447–2463.
[7] Q. Zheng, L. Li, M. Liu, B. Huang, N. Zhang, R. Mehmood, K. Nan, Q. Li, W. Chen, S. Lin, In situ scavenging of mitochondrial ROS by anti-oxidative MitoQ/hyaluronic acid nanoparticles for environment-induced dry eye disease therapy, Chem. Eng. J. 398 (2020) 125621.
[8] R.R. Mohan, D. Kempuraj, S. D'Souza, A. Ghosh, Corneal stromal repair and regeneration, Prog. Retin. Eye Res. 91 (2022) 101090.
[9] E.M. Espana, D.E. Birk, Composition, structure and function of the corneal stroma, Exp. Eye Res. 198 (2020) 108137.
[10] S. Lin, C. Ge, D. Wang, Q. Xie, B. Wu, J. Wang, K. Nan, Q. Zheng, W. Chen, Overcoming the anatomical and physiological barriers in topical eye surface medication using a peptide-decorated polymeric micelle, ACS Appl. Mater. Interfaces 11 (43) (2019) 39603–39612.
[11] D. Wang, B. Huang, C. Zhu, L. Wang, J. Jin, J. Tan, Q. Li, S. Xiang, K. Nan, S. Lin, Efficiency encapsulation of FK506 with new dual self-assembly multi-hydrophobic-core nanoparticles for preventing keratoplasty rejection, Adv. Healthcare Mater. 12 (21) (2023) 2203242.
[12] Q. Zheng, C. Ge, K. Li, L. Wang, X. Xia, X. Liu, R. Mehmood, J. Shen, N. Kaihui, W. Chen, S. Lin, Remote-controlled dexamethasone-duration on eye-surface with a micelle-magnetic nanoparticulate co-delivery system for dry eye disease, Acta Pharm. Sin. B 14 (8) (2024) 3730–3745.
[13] K. Glover, D. Mishra, S. Gade, L.K. Vora, Y. Wu, A.J. Paredes, R.F. Donnelly, T.R. R. Singh, Microneedles for advanced ocular drug delivery, Adv. Drug Deliv. Rev. 201 (2023) 115082.
[14] W. Park, V.P. Nguyen, Y. Jeon, B. Kim, Y.X. Li, J. Yi, H. Kim, J.W. Leem, Y.L. Kim, D.R. Kim, Y.M. Paulus, C.H. Lee, Biodegradable silicon nanoneedles for ocular drug delivery, Sci. Adv. 8 (13) (2022) eabn1772.
[15] A. Than, C.H. Liu, H. Chang, P.K. Duong, C.M.G. Cheung, C.J. Xu, X.M. Wang, P. Chen, Self-implantable double-layered micro-drug-reservoirs for efficient and controlled ocular drug delivery, Nat. Commun. 9 (1) (2018) 4433.
[16] E. Ivakhnitskaia, V. Souboch, V. Dallacasagrande, K. Mizerska, E. Souboch, J. Sarkar, V.H. Guaiquil, K.Y. Tseng, H. Hirata, M.I. Rosenblatt, Benzalkonium chloride, a common ophthalmic preservative, compromises rat corneal cold sensitive nerve activity, Ocul. Surf. 26 (2022) 88–96.
[17] M. Thacker, A. Sahoo, A.A. Reddy, K.K. Bokara, S. Singh, S. Basu, V. Singh, Benzalkonium chloride-induced dry eye disease animal models: current understanding and potential for translational research, Indian J. Ophthalmol. 71 (4) (2023) 1256–1262.
[18] M.H. Goldstein, F.Q. Silva, N. Blender, T. Tran, S. Vantipalli, Ocular benzalkonium chloride exposure: problems and solutions, Eye 36 (2) (2022) 361–368.
[19] C. Baudouin, A. Labbe, H. Liang, A. Pauly, F. Brignole-Baudouin, Preservatives in eyedrops: the good, the bad and the ugly, Prog. Retin. Eye Res. 29 (2010) 312–334.
[20] A. Pauly, E. Brasnu, L. Riancho, F. Brignole-Baudouin, C. Baudouin, Multiple endpoint analysis of BAC-preserved and unpreserved antiallergic eye drops on a 3D-reconstituted corneal epithelial model, Mol. Vis. 17 (2011) 745–755.
[21] M.Y. Kahook, R. Noecker, Quantitative analysis of conjunctival goblet cells after chronic application of topical drops, Adv. Ther. 25 (8) (2008) 743–751.
[22] M.Y. Kahook, R.J. Noecker, Comparison of corneal and conjunctival changes after dosing of travoprost preserved with sofZia, latanoprost with 0.02% benzalkonium chloride, and preservative-free artificial tears, Cornea 27 (3) (2008) 339–343.
[23] Y.H. Kim, J.C. Jung, S.Y. Jung, S. Yu, K.W. Lee, Y.J. Park, Comparison of the efficacy of fluorometholone with and without benzalkonium chloride in ocular surface disease, Cornea 35 (2) (2016) 234–242.
[24] N. Nagai, T. Murao, N. Okamoto, Y. Ito, Comparison of corneal wound healing rates after instillation of commercially available latanoprost and travoprost in rat debrided corneal epithelium, J. Oleo Sci. 59 (3) (2010) 135–141.
[25] M.I. Baker, S.P. Walsh, Z. Schwartz, B.D. Boyan, A review of polyvinyl alcohol and its uses in cartilage and orthopedic applications, J. Biomed. Mater. Res. B Appl. Biomater. 100 (5) (2012) 1451–1457.
[26] K. Peng, L.K. Vora, I.A. Tekko, A.D. Permana, J. Dominguez-Robles, D. Ramadon, P. Chambers, H.O. McCarthy, E. Larraneta, R.F. Donnelly, Dissolving microneedle patches loaded with amphotericin B microparticles for localised and sustained intradermal delivery: potential for enhanced treatment of cutaneous fungal infections, J. Contr. Release 339 (2021) 361–380.
[27] S.J. Chen, C.J. Lee, T.B. Lin, H.J. Liu, S.Y. Huang, J.Z. Chen, K.W. Tseng, Inhibition of ultraviolet B-induced expression of the proinflammatory cytokines TNF-alpha and VEGF in the cornea by fucoxanthin treatment in a rat model, Mar. Drugs 14 (1) (2016) 13.
[28] A. Hughes, A schematic eye for the rat, Vis. Res. 19 (5) (1979) 569–588.
[29] A.V. Ljubimov, M. Saghizadeh, Progress in corneal wound healing, Prog. Retin. Eye Res. 49 (2015) 17–45.
[30] M. Yazdani, K.B.P. Elgstøen, H. Rootwelt, A. Shahdadfar, Ø.A. Utheim, T. P. Utheim, Tear metabolomics in dry eye disease: a review, Int. J. Mol. Sci. 20 (15) (2019) 3755.
[31] E.M. Espana, D.E. Birk, Composition, structure and function of the corneal stroma, Exp. Eye Res. 198 (2020) 108137.
[32] D. Tiedemann, Z.A. Mouhammad, T.P. Utheim, D.A. Dartt, S. Heegaard, G. Petrovski, M. Kolko, Conjunctival goblet cells, the overlooked cells in glaucoma treatment, J. Glaucoma 28 (4) (2019) 325–333.
[33] K. Fukuda, Corneal fibroblasts: function and markers, Exp. Eye Res. 200 (2020) 108229.
[34] S.S. Chaurasia, R.R. Lim, R. Lakshminarayanan, R.R. Mohan, Nanomedicine approaches for corneal diseases, J. Funct. Biomater. 6 (2) (2015) 277–298.
[35] O. Weijtens, R.C. Schoemaker, F.P. Romijn, A.F. Cohen, E.G. Lentjes, J.C. van Meurs, Intraocular penetration and systemic absorption after topical application of dexamethasone disodium phosphate, Ophthalmology 109 (10) (2002) 1887–1891.
[36] C.S. Medeiros, G.K. Marino, M.R. Santhiago, S.E. Wilson, The corneal basement membranes and stromal fibrosis, Investig. Ophthalmol. Vis. Sci. 59 (10) (2018) 4044–4053.
[37] E. Arranz-Marquez, A. Katsanos, V.P. Kozobolis, A.G.P. Konstas, M.A. Teus, A critical overview of the biological effects of mitomycin C application on the cornea following refractive surgery, Adv. Ther. 36 (4) (2019) 786–797.
[38] P. Gain, R. Jullienne, Z. He, M. Aldossary, S. Acquart, F. Cognasse, G. Thuret, Global survey of corneal transplantation and eye banking, JAMA Ophthalmol 134 (2) (2016) 167–173.
[39] F. Senobari, S.S. Abolmaali, G. Farahavr, A.M. Tamaddon, Targeting inflammation with hyaluronic acid-based micro- and nanotechnology: a disease-oriented review, Int. J. Biol. Macromol. 280 (2024) 135923.
[40] I. Saha, V.K. Rai, Hyaluronic acid based microneedle array: recent applications in drug delivery and cosmetology, Carbohydr. Polym. 267 (2021) 118168.
[41] Q. Bao, X. Zhang, Z. Hao, Q. Li, F. Wu, K. Wang, Y. Li, W. Li, H. Gao, Advances in polysaccharide-based microneedle systems for the treatment of ocular diseases, Nano-Micro Lett. 16 (1) (2024) 268.
[42] C. Wu, Q. Yu, C. Huang, F. Li, L. Zhang, D. Zhu, Microneedles as transdermal drug delivery system for enhancing skin disease treatment, Acta Pharm. Sin. B 14 (12) (2024) 5161–5180.
[43] L.J. Kang, J. Yoon, J.G. Rho, H.S. Han, S. Lee, Y.S. Oh, H. Kim, E. Kim, S.J. Kim, Y. T. Lim, J.H. Park, W.K. Song, S. Yang, W. Kim, Self-assembled hyaluronic acid nanoparticles for osteoarthritis treatment, Biomaterials 275 (2021) 120967.
[44] Y. Lin, J.C. Xu, Y.H. Dong, Y. Wang, C.H. Yu, Y.H. Li, C.L. Zhang, Q.M. Chen, S. Chen, Q. Peng, Drug-free and non-crosslinked chitosan/hyaluronic acid hybrid hydrogel for synergistic healing of infected diabetic wounds, Carbohydr. Polym. 314 (2023) 120962.
[45] J.J. Chae, J.H. Jung, W. Zhu, B.G. Gerberich, M.R.B. Fard, H.E. Grossniklaus, C. R. Ethier, M.R. Prausnitz, Drug-free, nonsurgical reduction of intraocular pressure for four months after suprachoroidal injection of hyaluronic acid hydrogel, Adv. Sci. 8 (2) (2021) 2001908.
[46] C. Wang, Y. Pang, Nano-based eye drop: topical and noninvasive therapy for ocular diseases, Adv. Drug Deliv. Rev. 194 (2023) 114721.
[47] T.J. Shah, M.D. Conway, G.A. Peyman, Intracameral dexamethasone injection in the treatment of cataract surgery induced inflammation: design, development, and place in therapy, Clin. Ophthalmol. 12 (2018) 2223–2235.
[48] G.R. Snibson, J.L. Greaves, N.D. Soper, J.M. Tiffany, C.G. Wilson, A.J. Bron, Ocular surface residence times of artificial tear solutions, Cornea 11 (1992) 288–293.
[49] T. Kojima, T. Nagata, H. Kudo, W.G.K. Muller-Lierheim, G.B. van Setten, M. Dogru, K. Tsubota, The effects of high molecular weight hyaluronic acid eye drop application in environmental dry eye stress model mice, Int. J. Mol. Sci. 21 (10) (2020) 3516.
[50] C. Ni, Z. Zhang, Y. Wang, Z. Zhang, X. Guo, H. Lv, Hyaluronic acid and HA-modified cationic liposomes for promoting skin penetration and retention, J. Contr. Release 357 (2023) 432–443.

[51] D. Huang, Y.S. Chen, I.D. Rupenthal, Overcoming ocular drug delivery barriers through the use of physical forces, Adv. Drug Deliv. Rev. 126 (2018) 96–112.
[52] R.R. Mohan, A.E. Hutcheon, R. Choi, J. Hong, J. Lee, R.R. Mohan, R. Ambrosio Jr., J.D. Zieske, S.E. Wilson, Apoptosis, necrosis, proliferation, and myofibroblast generation in the stroma following LASIK and PRK, Exp. Eye Res. 76 (2003) 71–87.
[53] O.M. Hassan, A.V. Farooq, K. Soin, A.R. Djalilian, J.H. Hou, Management of corneal scarring secondary to herpes zoster keratitis, Cornea 36 (2017) 1018–1023.
[54] S.L. Wilson, A.J. El Haj, Y. Yang, Control of scar tissue formation in the cornea: strategies in clinical and corneal tissue engineering, J. Funct. Biomater. 3 (2012) 642–687.
[55] D.H. Dang, K.M. Riaz, D. Karamichos, Treatment of non-infectious corneal injury: review of diagnostic agents, therapeutic medications, and future targets, Drugs 82 (2) (2022) 145–167.
[56] A.T. Fung, T. Tran, L.L. Lim, C. Samarawickrama, J. Arnold, M. Gillies, C. Catt, L. Mitchell, A. Symons, R. Buttery, L. Cottee, K. Tumuluri, P. Beaumont, Local delivery of corticosteroids in clinical ophthalmology: a review, Clin. Exp. Ophthalmol. 48 (3) (2020) 366–401.
[57] M. Chen, X.L. Li, J.K. Liu, Y. Han, L.Y. Cheng, Safety and pharmacodynamics of suprachoroidal injection of triamcinolone acetonide as a controlled ocular drug release model, J. Contr. Release 203 (2015) 109–117.
[58] B.M. Rauck, T.R. Friberg, C.A.M. Mendez, D. Park, V. Shah, R.A. Bilonick, Y. D. Wang, Biocompatible reverse thermal gel sustains the release of intravitreal bevacizumab in vivo, Investig. Ophthalmol. Vis. Sci. 55 (1) (2014) 469–476.